



# Development of a test bench for lithium-ion battery evaluation: Towards high-performance battery management

Leonardo de Souza Takehana<sup>1</sup>, Renato Vilela Lopes<sup>1</sup>, Camilo Andres Villarraga Solis<sup>1</sup>, André Murilo de Almeida Pinto<sup>2</sup>, Walter Paschoal Pereira<sup>1</sup>

<sup>1</sup>Faculty UnB Gama, University of Brasilia Área Especial de Indústria Projeção A Setor Leste, CEP: 72.444-240, Gama/Distrito Federal, Brazil

<sup>2</sup>Federal University of Lavras

Trevo Rotatório Professor Edmir Sá Santos, CEP: 37203-202, Lavras/MG

leonardotakehana@gmail.com, rvlopes@unb.br, camilo.solis@aluno.unb.br, andremurilo@gmail.com, walterpaschoal@icloud.com

**Abstract.** Developing efficient, high-performance battery management systems requires an experimental bench capable of real-time data acquisition for various battery parameters. This paper details the development of an experimental bench, designed for efficient and safe testing of individual cells or cell sets. Notably, this proposed configuration is more cost-effective than existing market options. The bench facilitates real-time data acquisition of battery parameters by utilizing the PCI-DAS6013 analog acquisition board from Measurement Computing and integrated with Simulink Desktop's real-time environment. Furthermore, it incorporates power resistors, relay modules, and a controlled bench power supply for precise battery charging and discharge control. The setup's versatility extends to testing diverse battery operating conditions by applying varying current profiles during discharge.

**Keywords:** Battery management system, real-time data acquisition, battery testing, Simulink.

## 1 Introduction

The environmental challenges of the modern world drive the development of clean energy and justify the exponential growth of the global market for electrically powered vehicles over the past decade [1]. This transition aims to reduce greenhouse gas emissions, decrease reliance on fossil fuels, and stimulate technological innovation to build a more sustainable future. One of the most crucial subsystems in electric vehicle development is known as the Battery Management System (BMS). This system is responsible for monitoring, controlling, and protecting the batteries, optimizing vehicle performance and energy efficiency while ensuring maximum utilization and extended lifespan of the batteries [2].

However, due to the complicated electrochemical dynamics of the batteries and electrical coupling with other components, only voltage, current, and temperature monitoring is insufficient to result in a high-performance BMS [3]. Thus, estimating and monitoring accurately and robustly internal states constitute a fundamental approach to advanced battery management. Therefore, BMS should also estimate the state of charge, state of health, and state of functionality, balancing the cells, determining the remaining life, protecting cells, performing thermal management, controlling the load/discharge, diagnosing failures, and ensuring communication with external modules [4]. All of these tasks lead to the need for the development of sophisticated monitoring algorithms that represent a commitment between robustness, accuracy, adaptability, and hardware applicability [5].

In this sense, developing a high-performance BMS requires obtaining accurate mathematical models to describe the dynamic behavior of batteries [4]. These models can only be obtained through an experimental test set to acquire battery performance under various conditions. Additionally, the parameter adjustment task of these different estimation algorithms is usually based on experimental measurements, and the experimental data's accuracy directly influences the logical consistency and completeness of the analysis pertaining to battery characteristics. This influence subsequently extends to the precision and dependability of the battery model, culminating in an

impact on the operational efficacy of the BMS [5].

In this context, it is essential to have an appropriate experimental battery test platform that allows controlled charge and discharge tests and precisely collects the voltage, current, and cell temperature data. In the literature, several works use an experimental bench to perform tests to collect battery data. However, in most of these works, the goal is theoretical development, and little or no description of how to build these experimental benches is provided, or commercial experimental benches are used [6], [7], [8], [9]. However, the experimental platforms available on the market are usually very expensive and intended for testing in high-capacity batteries. This cost makes it unfeasible to acquire these platforms for research groups beginning their studies in batteries or wishing to conduct initial studies in small-capacity batteries.

Thus, this paper presents a methodology for constructing an experimental battery test platform to perform charge and discharge tests on batteries under different operating conditions with safety and efficiency. The main objective is to provide a practical and accessible guide to researchers and students that allow them to replicate this experimental bench using low-cost materials. This initiative is expected to contribute to technological advances and make it easier to understand the internal properties of batteries that can improve performance and durability.

This paper is organized as follows. First, the description of the experimental bench and the construction methodology are presented in Section 2. Some experimental results are presented in Section 3 to demonstrate the functionality of the proposed experimental bench. The paper ends with conclusions and future works in section 4.

## 2 Design and construction of the experimental battery test platform

This section presents the main design steps and details of the construction procedure of the experimental battery test platform. This experimental framework's main requirement is to perform charge and discharge tests on individual cells or cell packs while concurrently enabling the accurate data collection of voltage, current, and cell temperature. The architecture presented in Figure 1 is proposed to attend to these specifications, and each component will be described in the next subsections.

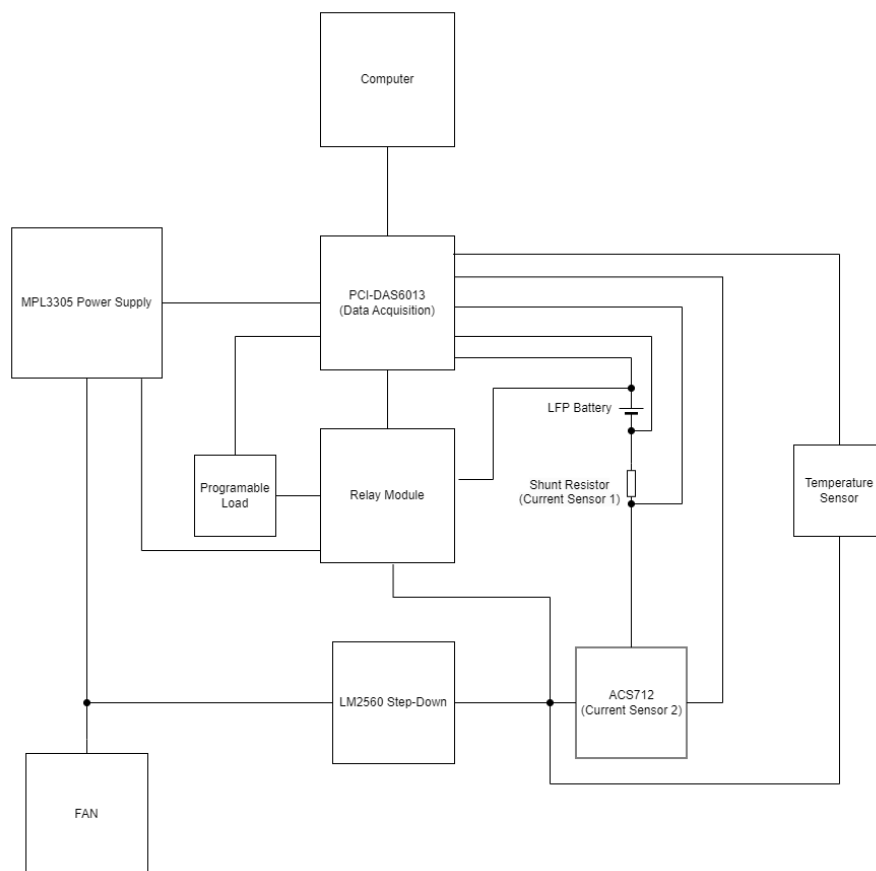


Figure 1. Experimental Bench Schematic

## 2.1 Computer and Data Acquisition

A computer featuring a 13th-generation Intel Core i7 CPU and 32GB of RAM, operating on Windows 10, is responsible for supervising the complete real-time testing procedure. This task is accomplished by utilizing the real-time Simulink desktop environment within the Matlab software. The data acquisition from sensors positioned on the experimental platform and the respective conversion of analog signs into digital is performed by the PCI-DAS6013 data acquisition board manufactured by the Measurement Computing company and was chosen for having full compatibility with the Real-Time Simulink Desktop.

## 2.2 Power Supply

The power supply's primary role entails furnishing energy to the battery cells and thus carrying out the battery charging process. The proposed experimental bench used the power supply MPL3305 featuring adjustable voltage and short-circuit protection and manufactured by Minipa company. In this model, the power supply operates in constant current mode when the battery is discharged and well below the charging voltage. It transitions to constant voltage mode as the battery approaches its fully charged state. Over time, the charging current diminishes toward zero.

## 2.3 Voltage Measurement

The voltages across the experimental platform are measured using the PCI-DAS6013 board, meticulously calibrated using Measurement Computing's Instacal software. These measurements are seamlessly integrated into Simulink through the Simulink Desktop Real-Time toolbox. However, the signals obtained from the board often demonstrate notable noise levels. As a countermeasure, the signal directed towards Simulink undergoes discrete low-pass filtering employing the transfer function  $\frac{1}{s+1}$  within a dedicated Simulink block. This filtration process eliminates high-frequency components inherent in the signal, resulting in a more refined and resilient output that is less susceptible to external interference.

## 2.4 Current Measurement

Battery current measurement is crucial to obtain a high-performance BMS because many internal battery parameters are estimated from the current entering or leaving the battery pack with respect to time. Thus, the proposed experimental bench uses two forms to measure the current. The first form uses a Hall effect current sensor. The sensor chosen was the ACS712, powered by the 5V output from the acquisition board. This sensor possesses the capability to conduct current measurements of up to 30A.

The second form performs the current measurement through a shunt resistor. This method measures the current indirectly, monitoring the voltage drop in a resistor connected in series with the battery. Thus, by knowing the resistance value and the voltage drop measured by the acquisition board, it becomes possible to calculate the current passing through the resistor using Ohm's law. On the proposed bench was used a 0.22Ω, 10W resistor.

It is important to highlight that in future work, these two current measurements will be combined using Kalman's filter algorithm for a more accurate estimation.

## 2.5 Temperature Measurement

Temperature measurement necessitates the utilization of an NTC thermistor, renowned for its resistance decreasing as the temperature rises. This project selected a thermistor with a reference resistance of 10kΩ at 25°C and a β coefficient of 3900K. The computation of temperature from resistance entails the application of the Steinhart-Hart equation:

$$\frac{1}{T} = \frac{1}{T_0} + \frac{1}{\beta} \cdot \ln \left( \frac{R_t}{R_0} \right) \quad (1)$$

where  $T$  represents sensor temperature,  $T_0$  is the reference temperature,  $\beta$  is the thermistor coefficient,  $R_t$  is the sensor resistance, and  $R_0$  is the reference resistance. The thermistor was part of a resistive voltage divider circuit, alongside a 10kΩ resistor  $R_1$ . This setup facilitated calculating the thermistor value based on input and output voltage. As the voltage divider equation is given by:

$$V_o = V_i \cdot \frac{R_1}{R_1 + R_t} \quad (2)$$

Isolating  $R_t$  yields:

$$R_t = \frac{V_i}{V_o} \cdot R_1 - R_1 \quad (3)$$

Substituting the equation 3 in equation 1, it is possible to obtain the temperature value.

## 2.6 Programmable Load

The battery discharge process is extremely important for characterizing batteries. Numerous experimental tests necessitate subjecting batteries to discharge at a constant current magnitude. This controlled discharge procedure aids in obtaining detailed insights into the battery's performance and behavior under specific conditions. However, a strategy is required to sink the current and absorb the energy drained from the batteries in the discharge process. The circuit that performs this task is called Programmable Load.

This work designed this circuit using a pair of IRF3205 MOSFETs in parallel, controlled by a digital output from the PCI-DAS6013 board. This arrangement allowed Simulink to generate a PWM signal for activating the MOSFETs. The board's output was connected to a first-order low-pass filter to produce a voltage signal based on the received pulses. This generated current  $I_d$  flows through the MOSFETs in series with a low-value resistor. This configuration enables capturing the voltage drop across the resistor and measuring the current passing through the circuit. The schematic of this circuit can be seen in Figure 2.

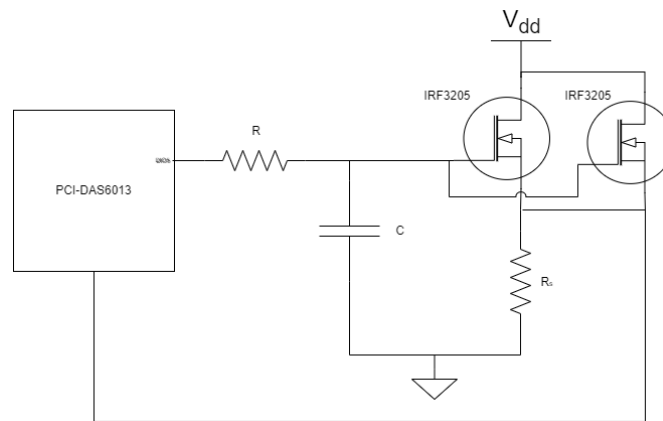


Figure 2. Programmable load schematic

The mathematical representation of this circuit enables the straightforward derivation of the subsequent transfer function.

$$G(s) = \frac{88}{0.15s^2 + 1.15s + 1} \quad (4)$$

where the numerator signifies the transconductance of the MOSFET within the operational zone, and the denominator is a convolution of  $0.15s + 1$ , the value of the input circuit's RC filter, and  $s + 1$ , the low-pass filter implemented via software for noise reduction. This arrangement allows the incorporation of a PID controller to maintain the intended current level. The PID controller is structured as follows

$$G_c(s) = K_p \left( 1 + \frac{1}{T_i s} + T_d s \right) \quad (5)$$

This work adjusted the controller parameters through the IMC-Based PID Procedure [10]. Thus, the parameters obtained were  $K_p = 0.0057$ ,  $T_i = 1.4846$ , and  $T_d = 0.1304$ . This PID controller was implemented in the Simulink environment. The projected Programmable Load can discharge batteries with a current of up to 5A.

## 2.7 Relay Module

For battery charging and discharging control, a 4-channel relay module was utilized under the command of Simulink. The arrangement encompasses a logical protocol to avert concurrent activation of both modes. Users can initiate these links through switch blocks: the initial relay guides power from the workbench power supply to the battery, and the second channel drains energy from the battery via the programmable load. This system still plays an important security role. The tests automatically turn off when the battery voltage reaches a maximum or minimum value. These values are determined as a function of the battery model used in the tests and are obtained through the battery datasheet provided by the manufacturer.

## 2.8 LM2560 Step-Down

Diverse devices necessitate distinct voltage levels in the proposed test bench configuration to ensure optimal operation. For example, the fan necessitates a voltage of 12V, whereas the relay module, temperature, and current sensors mandate a 5V power supply. Within this study, the decision was taken to employ the LM2560 Step-Down Converter. This particular component offers the notable advantage of precise voltage adjustment facilitated by a potentiometer. This adjustment regulates the 12V input to yield a meticulous 5V output. Consequently, the sensors are precisely calibrated, acknowledging their responsiveness to input voltage fluctuations and enhancing measurement accuracy. Notably, this solution simplifies the entire system, necessitating only a singular power source for the comprehensive test bench setup.

Considering user safety and circuit safeguarding, all components have been enclosed within a box featuring a fan. This fan regulates and upholds the internal temperature at appropriate levels. The connection of the internal circuits to the box and PCI-DAS6013 acquisition board through a cable terminating a DB15 connector. Furthermore, including four banana connectors simplifies linking a Minipa MPL-3305 bench power supply and the battery for measurement purposes. This arrangement is presented in Figures 3(a) and 3(b) to illustrate the open and closed box, respectively.

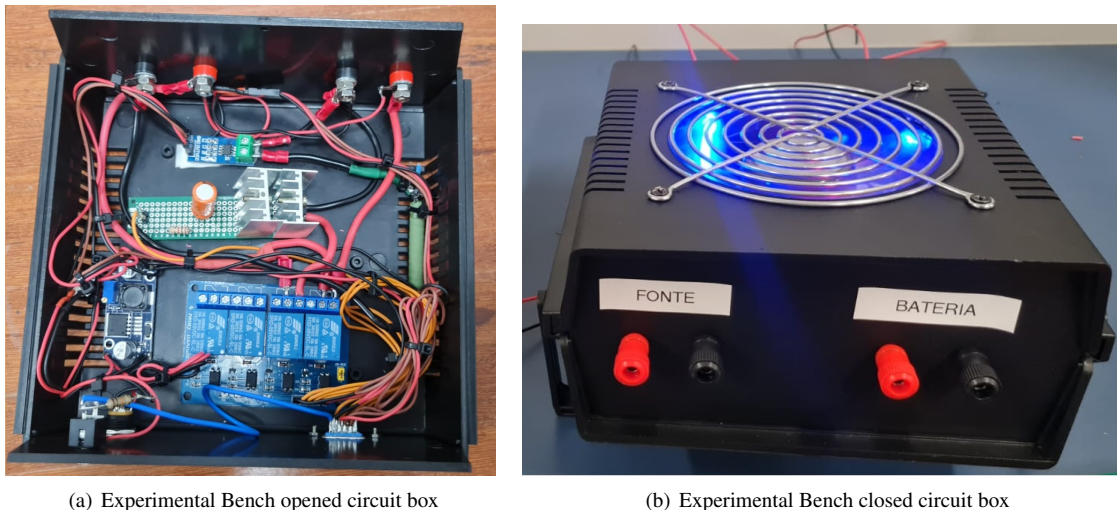
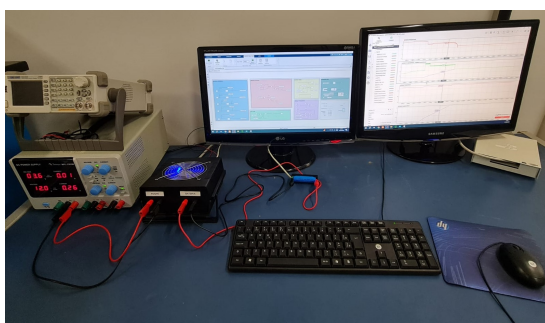


Figure 3. Sensors and electronic components of the experimental bench.

The complete setup of the proposed experimental bench is shown in Figure 4(a), and Table 1 presents the cost of implementation. The manufacturing process cost was not considered because it was accomplished in the institution's laboratory.



(a) Proposed experimental bench.

Table 1. List of Components and Costs

Description	Price (\$)*
Computer	1843.45
PCI-DAS6013 Acquisition Board	571.11
Minipa MPL3305 Bench Power Supply	452.46
Sensors and Components	70.23
LFP 2C 1500mAh Battery	8.52
<b>Total</b>	<b>\$ 2945.77</b>

(b) \* US Dollar Quote: 08/08/2023 (\$1,00 = R\$4,91)

Figure 4. Proposed experimental bench and implementation cost.

### 3 Results

This section presents experimental results obtained with the setup proposed in Figure 4(a). It is paramount to emphasize that these initial experiments were conducted just to assess the functionality of the configuration in question, devoid of adherence to pre-established protocols or any particular objectives.

These experiments utilized a lithium iron phosphate battery (LFP) of the 18650 model. This model is characterized by the subsequent nominal specifications: 3.2V, 1.5 Ah, and 2C discharge rate. In all experiments, a sampling period of 10ms was used. Initially, the performance of the programmable load circuit was evaluated. For this, a previously charged battery discharge process was carried out, and the value of the 1.5A discharge current was specified. The result obtained can be observed in Figure 5. It can be observed that the integration of MOS-FETs and a PID controller for programmable discharging showcased the bench's capacity for controlled energy dissipation and can maintain the current value in the specified value. The system response time is considered satisfactory.

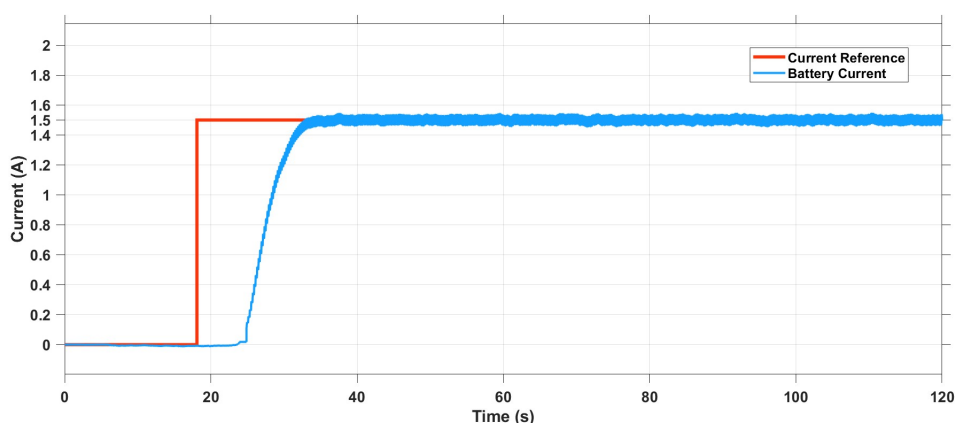


Figure 5. Programmable Load circuit performance in response to a unit step in the reference current value.

Additionally, the accuracy of the current measurement system was evaluated. The values obtained by the two measuring forms implemented were compared to values provided by a multimeter. This comparison yielded a variation of approximately two milliamperes, showcasing the high precision of the utilized system.

The following procedure was performed to evaluate a complete load and discharge process. Initially, the battery was linked to the system while discharged, displaying an open-circuit voltage of roughly 2.7V. Following this, the bench power supply was configured to 3.65V, prompting the commencement of the charging procedure until the charging current approached near-zero levels. Subsequently, an interval of approximately 30 minutes was noted, during which the battery's voltage was allowed to reach a state of stability. Consequently, a discharge sequence was set into motion, employing a consistent current until the quantity of discharged current corresponded precisely to the amount of current applied during the charging process. Within the discharge procedure, two distinct current values were designated to exemplify the potential for applying diverse current profiles to the experimental setup. Initially, a current magnitude of 1.5A was configured, followed by an adjustment to 1A. This feature is important to allow testing batteries under different operating conditions. The results are presented in Figure 6, and the change of the charging process, indicated by a negative current value, to the discharge process, represented by a positive current value, can be observed. The activation of charging or discharging was successfully implemented using Simulink.

It is also possible to note that the MPL3305 bench power supply demonstrated its effectiveness in controlling the charging process. By transitioning between constant current and constant voltage modes, the power supply ensured safe and controlled charging of the battery. Figure 6 also shows that NTC thermistor-based temperature measurement method effectively captures temperature changes within the system.

### 4 Conclusions

This article described all the steps involved in the design of an experimental battery testing bench. Experimental results using an LFP battery were presented as preliminary tests. The proposed configuration presented a cost of \$ 2945.77, which represents only a small percentage of the cost of a commercial experimental bench.

The proposed approach proved to be a versatile and effective platform for analyzing battery behavior, offering precise measurement and control capabilities for voltage, current, and temperature. Integrating advanced techniques, such as PID control and temperature measurement, enabled comprehensive investigations into battery



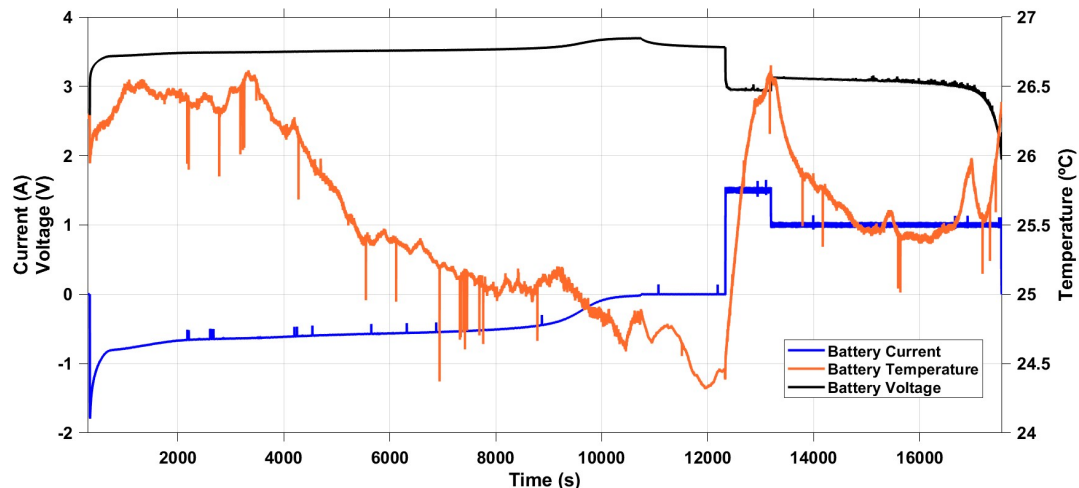


Figure 6. Results obtained in the charge and discharge process. Negative current values indicate the battery charge process, while positive values indicate the discharge process.

performance under varying conditions. The results obtained through the experiments validated the robustness of the system and its applicability in studying battery dynamics, making it a valuable asset for research, experimentation, and innovation in battery-related studies.

In future work will be developed a Kalman filter to combine the current measurement of the two sensors installed on the bench and thus obtain an estimate of the more accurate current. In addition, temperature sensors will be replaced for more accurate measurements.

## Acknowledgments

The authors acknowledge the financial support provided by Fundep – Rota 2030 and the Federal District Research Support Foundation (FAP-DF).

## References

- [1] N. Zhou, H. Liang, J. Cui, Z. Chen, and Z. Fang. A Fusion-Based Method of State-of-Charge Online Estimation for Lithium-Ion Batteries Under Low Capacity Conditions. *Frontiers in Energy Research*, vol. 9, 2021.
- [2] F. Z. Hui Pang. Experimental data-driven parameter identification and state of charge estimation for a li-ion battery equivalent circuit model. *Journal Energies*, pp. 10.3390/11051033, 2018.
- [3] Y. Che, Z. Deng, P. Li, X. Tang, K. Khosravinia, X. Lin, and X. Hu. State of health prognostics for series battery packs: A universal deep learning method. *Energy*, vol. 238, pp. 121857, 2022.
- [4] C. T. Da Silva, B. M. d. A. Dias, R. E. Araújo, E. L. Pellini, and A. A. M. Laganá. Battery Model Identification Approach for Electric Forklift Application. *Energies*, vol. 14, n. 19, pp. 6221, 2021.
- [5] R. Xiong, ed. *Battery Management Algorithm for Electric Vehicles*. Springer Singapore, Singapore, 2020.
- [6] X. C. H. C. J. D. J. Z. Liangqiang C. Yahui W. Research on online identification of lithium-ion battery equivalent circuit model parameters. *International Forum on Electrical Engineering and Automation (IFEAA)*, pp. 978–1–6654–6421, 2022.
- [7] S. W. Y. W. W. Z. Qiang F. Biao J. Experimental study on pulse discharge characteristics of square power lithium-ion battery. *Materials Science and Engineering Application M. Chen et al. (Eds.)*, pp. 10.3233/ATDE220520, 2022.
- [8] M. E. V. J. H. L. Alves C. Santos R. Estimation of lithium-ion battery model parameters using experimental data. *Federal University of Paraíba*, 2019.
- [9] H. A. M. A. Lipu M.S.H. Hannan M.A. A review of lithium-ion battery state of charge estimation and management system in electric vehicle applications: Challenges and recommendations. *Elsevier Ltd. All rights reserved*, pp. 1364–0321, 2017.
- [10] B. W. Bequette. *Process control: modeling, design, and simulation*. Prentice Hall Professional, 2003.